The Effects of Heat Treatment On Zircon Inclusions in Madagascar Sapphires

Wuyi Wang, Kenneth Scarratt, John L. Emmett, Christopher M. Breeding, and Troy R. Douthit

Zircon inclusions in sapphires from Madagascar were studied to investigate the effects of heat treatment on their gemological and spectroscopic features. Progressive decomposition of zircon and chemical reactions between zircon and the host sapphire occurred at temperatures between 1400°C and 1850°C. In unheated sapphires, transparent zircon inclusions displayed euhedral slightly elongated forms and clear interfaces with their corundum host. Most were confined within the host under relatively high pressures (up to 27 kbar), and showed evidence of natural radiation-related damage (metamictization). Subsolidus reactions (i.e., the decomposition of zircon into its component oxides without melting) of some zircon inclusions started at temperatures as low as 1400°C, as evidenced by the formation of baddeleyite (ZrO_2) and a SiO_2-rich phase. Differences in the degree of preexisting radiation damage are the most likely cause for the decomposition reactions at such relatively low temperatures. Melting of zircon and dissolution of the surrounding sapphire occurred in all samples at 1600°C and above. This resulted in the formation of both baddeleyite and a quenched glass rich in Al_2O_3 and SiO_2. From these data and observations, a systematic sequence of both modification and destruction of zircon inclusions with increasing temperature was compiled. This zircon alteration sequence may be used (1) as a gemological aid in determining whether a zircon-bearing ruby/sapphire has been heated, and (2) to provide an estimate of the heating temperature.

Because of the high demand for attractive sapphires and rubies, many different treatments have been applied to mid- and low-grade corundum to enhance color and clarity. On an atomic level, by modifying trace-element concentrations and defect configurations in the corundum crystal structure, selective light absorption in the visible spectrum can be changed to produce pleasant bodycolors and thus more valuable sapphires (see, e.g., Crowningshield, 1966; Beesley, 1982; Emmett and Douthit, 1993). Heating traditionally has been one of the most common treatments and remains so today.

As would be expected, temperature is one of the most critical factors in the heat treatment of sapphire. Modern technology has allowed sapphires to be exposed to higher temperatures, has produced more dramatic color changes in shorter periods of time, and has expanded the range of material suitable for enhancement. With the recent development of the beryllium-diffusion process, treatment temperatures as high as 1850°C, near the melting point of corundum (2030°C–2050°C), have become common (Emmett et al., 2003).

Zircon ($ZrSiO_4$) is a common inclusion in Madagascar sapphires, which are important because they span the color spectrum (figure 1); stones from this locality may also be sourced for Be diffusion. Zircon is prevalent in corundum from many other geographic sources as well (see, e.g., Schwieger, 1990; Guo et al., 1996; Hughes, 1997; Rankin, 2002;

See end of article for About the Authors and Acknowledgments.
Gems & Gemology, Vol. 42, No. 2, pp. 134–150.

Figure 1. Natural sapphires, such as these 45 princess cuts from Madagascar, come in a broad range of colors. Nevertheless, the high demand for fine ruby and sapphire has led to a wide variety of treatments, of which heating to improve color and/or clarity is perhaps the most common. These sapphires have a total weight of 23.08 ct. Courtesy of Pala International, Fallbrook, California; photo © Jeff Scovil.

Rankin and Edwards, 2003). During heat treatment, included mineral crystals are subjected to the same conditions as the corundum host, but since they have different thermodynamic and chemical properties, they may expand, recrystallize, melt, or chemically react with the host corundum in very different ways that are dependent on the heating temperature, time, and other factors. Observation of destroyed or modified mineral inclusions using an optical microscope has long been used to identify heat-treated sapphires (see, e.g., Gübelin, 1973; Scarratt, 1983; Gübelin and Koivula, 1986; Cozar and de Vincente-Mingarro, 1995; Hughes, 1997). However, systematic descriptions of morphological changes in response to heating for specific mineral inclusions such as zircon are not widely available (Cozar and de Vincente-Mingarro, 1995; Rankin and Edwards, 2003).

Of particular concern in recent years, diffusion of a trace amount of beryllium (from several up to tens of parts per million) into corundum can lead to a fundamental change in bodycolor (Emmett et al., 2003). Although the diffusion coefficient of Be in corundum is higher than that of many other elements, diffusion of Be into corundum is still a very slow process. A very high temperature (~1800°C) is often necessary to process the stone in a reasonable amount of time, although Be diffusion may occur at lower temperatures. Using the morphology of zircon inclusions to estimate the heating temperature could minimize the number of samples that would have to be submitted for trace-element analysis.

MATERIALS AND METHODS

A total of 41 rough sapphires from Madagascar, ranging from 0.21 to 4.34 ct, were selected for this study based mainly on the possible occurrence of zircon inclusions. All of the samples were irregular in shape, and over half exhibited the flat morphology that is common for Madagascar sapphires. Most were from GIA's collection of specimens obtained directly from the Ilakaka area of Madagascar; the rest (slightly less than one-third) were purchased from reliable sources in the market. All were known to be natural and untreated by heat or any other method.

Twenty-five samples were heated to various temperatures so we could observe changes in their zircon inclusions; their properties and heating conditions are given in table 1. The remaining 16 were left unheated for comparison. After heating, most were pink or purplish pink of varying saturation, but some were near colorless or had slight blue or yellow hues. While we did note overall color changes, since the focus of this study was the zircon inclusions, we did not track color changes with temperature or attempt to control the atmosphere to achieve optimal coloration.

Heating experiments were carried out using a vertical furnace with an oxidizing atmosphere in the facilities of Crystal Chemistry, Brush Prairie, Washington. Target annealing temperatures varied from 1400°C to 1850°C. For each experimental run, two to three samples were heated at the target temperature in a high-purity alumina crucible for 5 hours; this time was considered adequate to reach

equilibrium conditions. To evaluate the effects of different heating durations, additional experiments at 1600°C and 1730°C were performed for 25 and 12 hours, respectively. During each run, the temperature was raised from room temperature to 1000°C at a rate of 300°C/hour, and then to the target temperature at a rate of 600°C/hour. Temperatures measured in this study are believed to be accurate to about ±1%, and fluctuation in each experimental run was less than ±10°C. After annealing at the target temperature for 5 hours, in most cases the temperature was then decreased to room temperature over a period of 4 hours. Following the heating experiments, all samples were ground on both sides to at least 0.5 mm depth to remove possible surface contamination, and then polished for observation and analysis.

TABLE 1. Heated (with experimental conditions) and unheated Madagascar sapphires studied for this report.

Sample no.	Weight (ct)	Thickness (mm)	Heating experiment		
			Temperature (˚C)	Duration (hours)	Environment
75965	0.65	1.07	1400	5	Oxidizing
75966	0.89	1.41		5	
75967	1.29	1.73		5	
65458	1.61	2.58	1450	5	Oxidizing
65459	1.12	2.06		5	
65460	1.05	2.50	1500	5	Oxidizing
65461	1.10	1.62		5	
65462	1.79	2.59	1550	5	Oxidizing
65463	0.96	2.16		5	
56016	1.88	3.76	1600	5	Oxidizing
56017	3.32	4.25		5	
75968	0.83	1.27		25	
75969	1.18	1.80		25	
75970	0.70	1.21		25	
56018	3.25	3.64	1680	5	Oxidizing
56019	2.82	nd[a]		5	
56020	2.03	2.23	1730	5	Oxidizing
56021	2.27	nd		5	
75971	0.35	0.91		12	
75972	0.64	1.14		12	
75973	0.75	2.15		12	
56022	2.94	3.49	1780	5	Oxidizing
56023	1.90	3.32		5	
56024	1.52	2.36	1850	5	Oxidizing
56025	4.34	nd		5	
56536	0.65	nd	Not treated		
75974	0.72	1.08			
75975	0.77	1.99			
75976	1.09	1.81			
76726	0.60	1.41			
76728	0.32	1.15			
76729	0.63	1.29			
76730	0.38	1.30			
76731	0.26	1.07			
76732	0.21	0.62			
76733	0.53	1.56			
76734	0.23	1.07			
76735	0.31	1.42			
76736	0.30	1.07			
76737	0.40	1.09			
76738	0.92	1.99			

[a] *nd = not determined.*

In two unheated and all the heated sapphires, the surface-reaching zircon inclusions were analyzed using a high-resolution analytical scanning electron microscope (LEO 1550 VP FESEM) equipped with an Oxford INCA Energy 300 energy-dispersive X-ray spectrometer (EDS) at the California Institute of Technology. A thin layer of carbon was coated over a polished surface of each sapphire to improve electrical conductivity. Since most zircon inclusions are very small and the decomposition products are even smaller, the results of quantitative elemental analysis were normalized. This way, a relative accuracy of better than 5% and a detection limit of better than 0.5 wt.% could be obtained. The analyses were performed using an accelerating voltage of 20 kV, a focused electron beam with a a spot size of 1–2 μm, and a beam current of 10 nA. Backscattered electron (BSE) images were obtained to provide a means of mapping areas in a sample that contained elements of different atomic weights.

Infrared absorption spectra of the host sapphire were recorded in the mid-infrared region (6000–400 cm^{-1}, 1.0 cm^{-1} resolution) at room temperature with a Thermo-Nicolet Nexus 670 Fourier-transform infrared (FTIR) spectrometer equipped with a KBr beam splitter and MCT-B detector. Prior to analysis, the samples were cleaned using an ultrasonic bath with pure acetone to remove surface contamination. A 2-mm-diameter center portion of each sample was selected for analysis, and the rest of the sample was shielded using a clean metal mask. A 6× beam condenser focused the incident beam through the sample, and a total of 256 scans (per spectrum) were collected to improve the signal-to-noise ratio.

Raman spectra of the zircon inclusions and their host sapphires were recorded at room temperature using a Renishaw 1000 Raman microspectrometer with a polarized Ar-ion laser at two different laser excitations (488.0 and 514.5 nm). The two lasers were used to help clarify the identity of some emission peaks (Raman scattering vs. luminescence). The instrument was calibrated against the first-order Raman shift of a type IIa diamond at 1332.5 cm^{-1}. Spectra were collected using a confocal

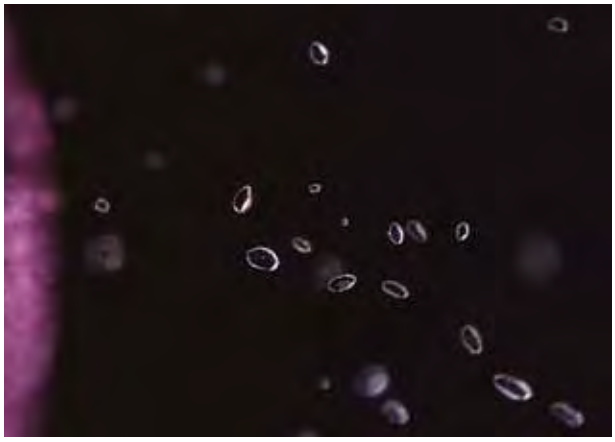

Figure 2. Discrete zircon inclusions were common in the Madagascar sapphires. With magnification, the interfaces between the zircon inclusions and their host sapphire were almost always clear and transparent, showing no frostiness or turbidity. The crystal faces were flat or somewhat rounded and shiny. Photomicrograph by W. Wang; magnified 90×.

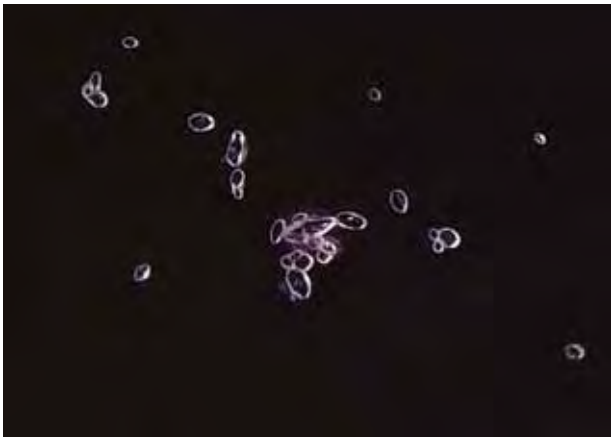

Figure 3. Clusters of zircon inclusions were present in many of the Madagascar sapphires. Aggregations usually consisted of less than 10 crystals, and no other minerals were observed as part of these clusters. In rare cases, up to 100 crystals were seen in a large cluster. Photomicrograph by W. Wang; magnified 90×.

system with a grating of 1800 grooves per mm, slit width of 50 μm, objective lens of 50×, and initial laser power of 20 mW. Up to 100 scans were accumulated to achieve a better signal-to-noise ratio. Raman spectra of the host sapphires were collected in the same orientation used for the inclusions by slightly moving the sample stage horizontally. Raman spectra of the zircon inclusions in both the unheated and heated sapphires were obtained by subtracting an appropriate percentage of the host sapphire spectrum (i.e., when Raman peaks from corundum disappeared entirely) from that collected directly from the inclusions.

In addition, to better evaluate the spectral features of the zircon inclusions, we analyzed two faceted free-standing zircons (one blue and one colorless) in several random directions. We also analyzed a euhedral purple zircon crystal that had well-developed prismatic morphology with the c-axis parallel, at 45°, and perpendicular to the laser polarization. The geographic sources of these single-crystal zircons are unknown.

RESULTS

Unheated Samples. In the 16 unheated sapphires, minor amounts of monazite and apatite were present, but zircon was the most common inclusion. Thirteen of the samples showed pink-purple coloration; the other three were colorless, blue, and greenish yellow. Abundant zircon inclusions were observed in the colorless and 11 of the pink samples.

Microscopic Observation. Typically, the unheated zircon inclusions were transparent with a slightly elongate crystal habit and well-developed {110} form, although many were slightly rounded. They ranged from less than 10 μm to about 100 μm in the longest dimension, though most were smaller than 50 μm. A few samples contained mostly individual inclusions (figure 2), while others displayed clusters (figure 3). The latter usually consisted of less than 10 zircon crystals and no other minerals; in two samples, they showed as many as 100 crystals. Generally, the inclusions were randomly distributed within the host sapphire, but three samples showed linear orientation to some extent. Even when viewed at up to 100× magnification, their interfaces with the host sapphire were almost always clear and transparent. The crystal faces of the zircons were flat or slightly rounded, and reflective. Some of the larger zircons crystals and clusters were accompanied by radial fractures in the surrounding corundum (figure 4); however, the depth of these fractures extending from the inclusion surface into the sapphire hosts was limited, with most no larger than the inclusion itself. Some were very subtle and could only be observed with carefully oriented lighting. Similar to the interface between the zircon inclusions and the host sapphire, these fractures were clean and smooth. No foreign material or apparent frosting was observed (again, see figure 4).

SEM-EDS Analysis. Seven pristine zircon inclusions in two unheated sapphires (nos. 75974 and

Figure 4. Radial fractures were often present around larger zircon inclusions. The depths of the fractures were limited, and most were close to the size of the inclusions and only rarely reached the surface of the host sapphire. Photomicrograph by W. Wang; magnified 112×.

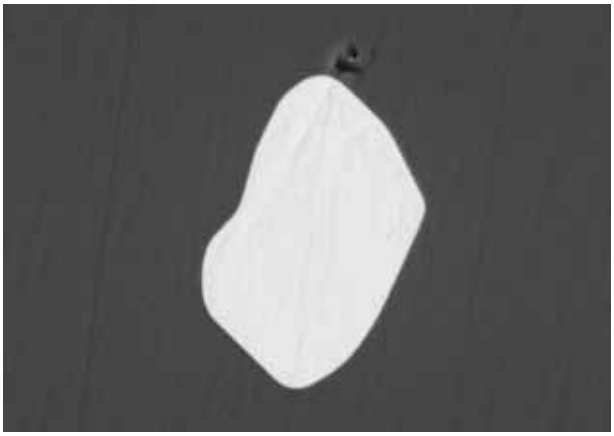

Figure 5. This backscattered electron image shows a uniform zircon crystal that has a sharp planar boundary with the surrounding host sapphire. Due to its high content of the heavy element zirconium, the zircon inclusion appears much brighter than the surrounding host sapphire. Image width 70 μm.

75975) were chemically analyzed using SEM-EDS (representative data in table 2). BSE images of inclusions exposed at the surface showed uniform zircon crystals with sharp planar or slightly rounded boundaries (figure 5) and no evidence of decomposition; a few displayed growth zoning. Chemical analysis revealed that these inclusions were nearly pure zircon ($ZrSiO_4$) with only minor amounts of HfO_2 (from less than the instrument detection limit up to ~2 wt.%).

Infrared Absorption Spectroscopy. The unheated host sapphires displayed few features in the mid-IR region other than a weak absorption at 3309 cm^{-1}

TABLE 2. Representative element concentrations (wt.% oxide) of zircon inclusions and of their reaction products after the heating experiments.

Sample no.	Heating temperature (°C)	Phase	Na_2O	MgO	Al_2O_3	SiO_2	K_2O	CaO	TiO_2	FeO	ZrO_2	Ce_2O_3	HfO_2
75974	Unheated	Zircon	–[a]	–	–	32.6	–	–	–	–	65.8	–	1.6
		Zircon	–	–	–	32.4	–	–	–	–	65.7	–	1.9
		Zircon	–	–	–	32.1	–	–	–	–	66.4	–	1.5
75975	Unheated	Zircon	–	–	–	32.8	–	–	–	–	67.2	–	–
		Zircon	–	–	–	32.4	–	–	–	–	67.7	–	–
75967	1400	Zircon	–	–	–	32.9	–	–	–	–	67.1	–	–
		Baddeleyite	–	–	1.7	9.4	–	–	–	–	87.6	–	1.4
65458	1450	Zircon	–	–	–	33.0	–	–	–	–	67.0	–	–
		Baddeleyite	–	–	1.9	21.2	–	–	–	–	76.9	–	–
75968	1600	Zircon	–	–	–	34.1	–	–	–	–	62.8	–	3.2
		Baddeleyite	–	–	1.0	–	–	–	–	–	96.0	–	3.1
75969	1600	Baddeleyite	–	–	–	–	–	–	–	–	95.1	–	4.9
		Melt	–	4.5	21.8	71.4	0.9	–	–	–	2.1	–	–
56018	1680	Baddeleyite	–	–	2.7	–	–	–	–	–	97.7	–	–
		Melt	3.2	–	18.4	54.8	–	4.2	2.5	–	16.9	–	–
56020	1730	Baddeleyite	–	–	–	–	–	–	–	–	98.6	–	1.4
		Melt	–	–	73.7	26.3	–	–	–	–	–	–	–
56023	1780	Baddeleyite	–	–	3.2	–	–	1.4	–	–	95.4	–	–
		Melt	0.2	3.2	28.6	41.7	–	14.7	2.5	0.2	8.4	0.5	–
56024	1850	Baddeleyite	–	–	–	–	–	–	–	–	100.0	–	–
		Melt	–	–	29.3	66.4	–	–	–	2.0	4.6	–	–

[a] – = not detected.

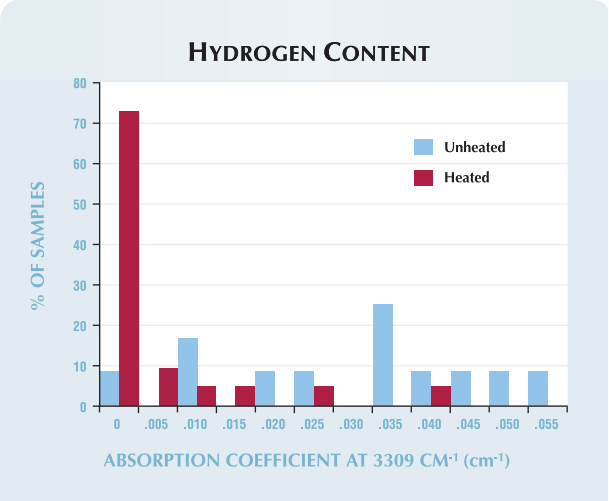

Figure 6. The hydrogen-related absorption coefficient at 3309 cm^{-1} was much stronger in the unheated sapphires from Madagascar than in the heated samples. Most of the latter, which were heated in an oxidizing environment, contained no structurally bonded hydrogen after treatment.

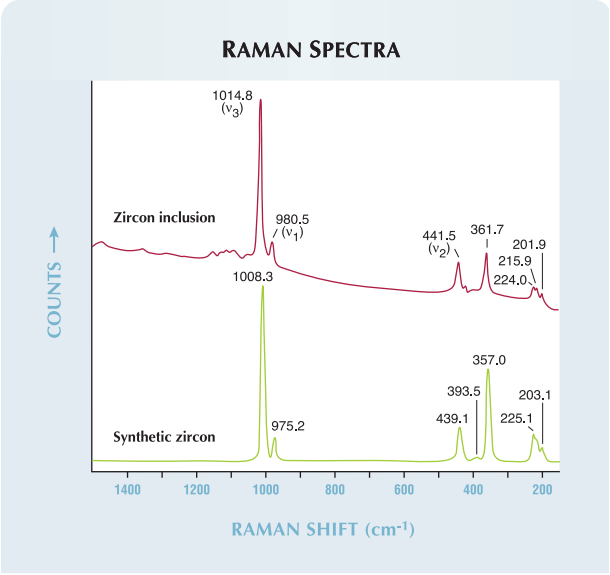

Figure 7. Strong Raman peaks overlying a relatively flat background were recorded in all analyzed zircon inclusions. Compared with synthetic end-member zircon (G. Rossman, pers. comm., 2006), a notable feature is the evident shifting of almost all Raman peaks.

produced by structurally bonded hydrogen. All but one of the unheated sapphires showed the 3309 cm^{-1} absorption, with intensity of the absorption coefficient varying from ~0.010 to ~0.055 cm^{-1} (figure 6). These data indicate that trace hydrogen is common in unheated Madagascar sapphires.

Raman Spectroscopy. Micro-Raman analysis produced some interesting information on the zircon inclusions. All displayed seven or eight peaks in the region of 1050–200 cm^{-1} (figure 7, top spectrum). These peaks were much broader and weaker in intensity than the characteristic Raman peaks of synthetic end-member zircon in the 1050–200 cm^{-1} region (again, see figure 7, bottom spectrum; G. Rossman, pers. comm., 2006; see also Nasdala et al., 2003). The peaks above 1020 cm^{-1} were also observed in the spectra from the blue and colorless free-standing zircons. Three peaks (ν_1—symmetric stretching, ν_2—symmetric bending, ν_3—antisymmetric stretching [again, see figure 7]; Griffith, 1969; Syme et al., 1977) were relatively sharp with full width at half maximum (FWHM) of 6.7–11.2 cm^{-1}, 13.6–18.4 cm^{-1}, and 10.1–13.5 cm^{-1}, respectively, at 514.5 nm laser excitation.

Most of the Raman peaks from the inclusions were shifted from the values of the two faceted free-standing zircon samples (figure 8). In particular, for the ν_3 mode, the Raman peaks in these free-standing zircons had a very limited range of variation (1007.8–1008.4 cm^{-1}). In the free-standing purple crystal tested in several orientations, we observed significant variations in peak intensities, but no shifting in peak positions. When the c-axis was parallel to the

Figure 8. Among the 23 analyzed inclusions in unheated sapphires, the Raman peaks of only two inclusions fell in positions similar to those of synthetic end-member zircon (G. Rossman, pers. comm., 2006) or unheated zircons analyzed in this study. All the other zircon inclusions exhibited much higher peak positions. In addition, a positive correlation was observed between peak positions. Similar positive relations were detected between other peaks (not shown).

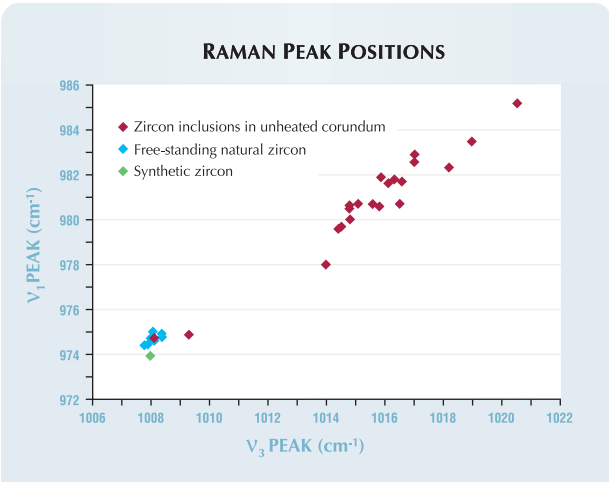

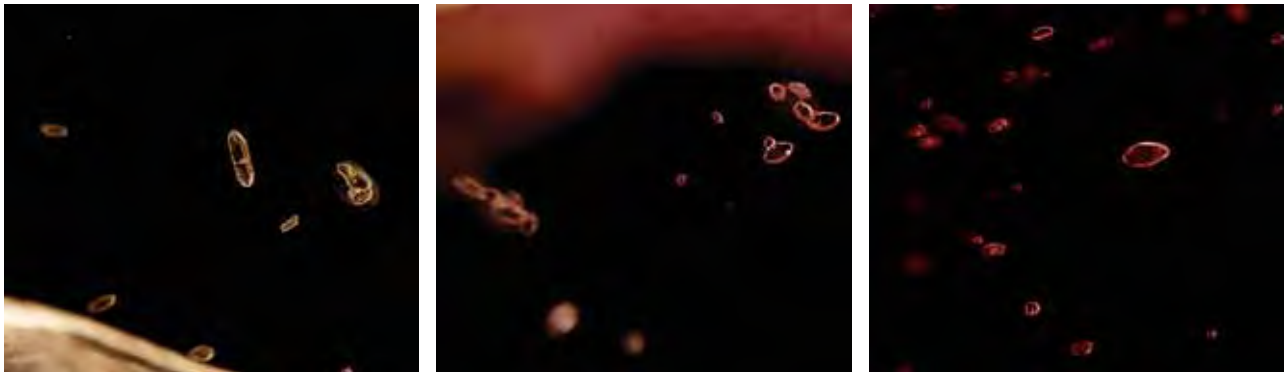

Figure 9. At or below 1500°C, the morphology of the zircon inclusions did not change noticeably (left, 1400°C [sample no. 75967]; center 1450°C [no. 65459]; right 1500°C [no. 65460]). However, in some zircons, portions of the interface between the inclusion and the host became slightly turbid or frosted, as did some fractures around the inclusions. Photomicrographs by W. Wang; magnified 100×.

vibrational direction of the incident laser beam, the ν_1 and ν_3 peaks almost disappeared entirely. The strongest intensities of ν_1 and ν_3 were observed when the c-axis was 45° to the vibrational direction. The three major peaks showed very limited positional variations when measured at different orientations (ν_1: 974.4–975.0 cm^{-1}; ν_2: 438.7–438.9 cm^{-1}; ν_3: 1007.8–1008.1 cm^{-1}). These values are similar to those from synthetic end-member zircon (again, see figure 7).

In contrast, of the 23 zircon inclusions in 12 unheated sapphires that were measured, only two fell within the positional ranges observed in the free-standing zircon samples. All the other inclusions yielded peaks that were shifted to much higher positions (e.g., ν_3: 1014–1021 cm^{-1}; again, see figure 8). The largest shift from ideal position was nearly 13 cm^{-1}. Similar peak shifting occurred for other peaks (ν_1, ν_2, and another major peak at ~360 cm^{-1}), and a clear positive correlation was observed among the peaks (e.g., ν_1 vs. ν_3 in figure 8). Multiple inclusions within the same sapphire also showed large variations in peak position. For example, in sample no. 75975, ν_3 of one zircon occurred at 1008.1 cm^{-1}, but two other inclusions had positions ranging from 1015.6 to 1017.7 cm^{-1}. Similar large variations for the position of ν_3 were observed in sample no. 76732 (1009.3 cm^{-1} and 1014.8–1015.1 cm^{-1}). Five zircon inclusions were analyzed in sample no. 76726, but the position of ν_3 showed only a very limited range of variation (1014.4–1016.5 cm^{-1}).

Heated Samples. *Visual Observation.* Color changes were observed in these sapphires after heat treatment, with a deeper pink color in some stones and lighter pink in others. As noted earlier, we did not track systematic variations in color with temperature. The zircon inclusions displayed distinct changes in crystal morphology after heating to suffi-

Figure 10. As the temperature was increased to 1550°C (left [sample no. 65462]), the frosted/turbid regions became larger and more noticeable. At 1600°C (center [no. 56017]), the surfaces of nearly all the zircon inclusions became noticeably frosted, and only a few transparent regions remained. At 1680°C (right [no. 56018]), the zircon crystals lost their original outlines, resulting in irregular shapes. Photomicrographs by W. Wang; magnified 100×.

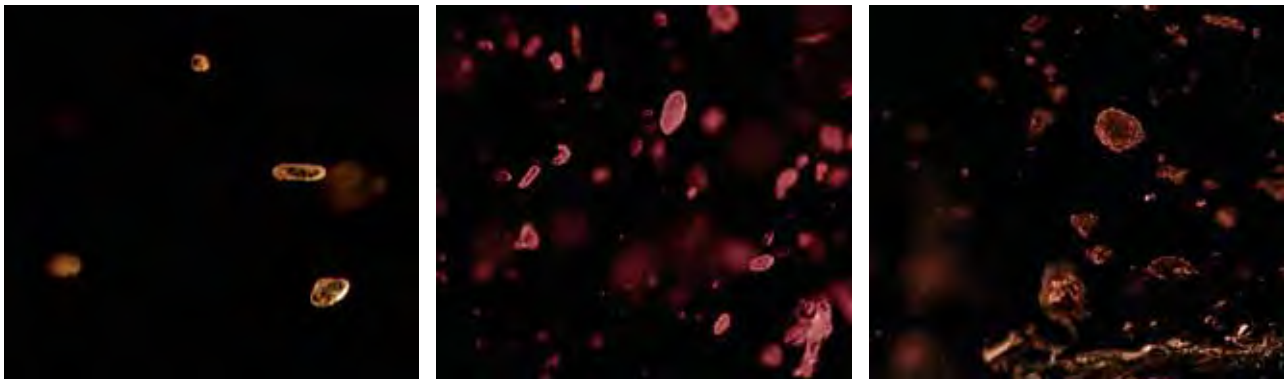

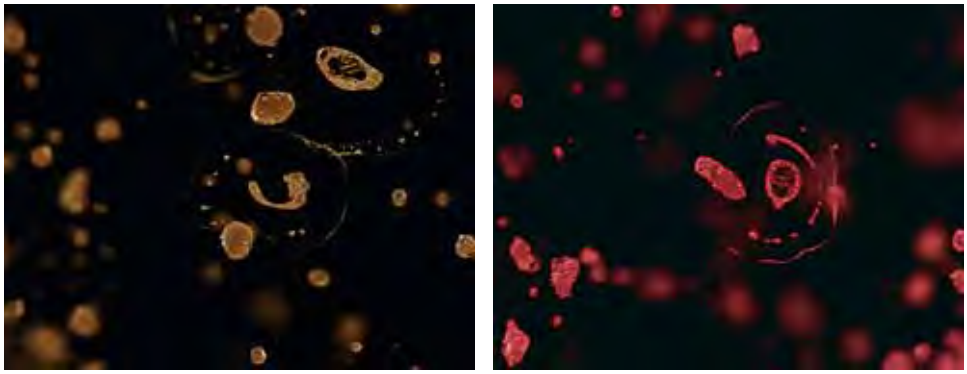

Figure 11. Melting and formation of discoid fractures began around 1730°C (left, heated for 12 hours [sample no. 75973]) and intensified as the temperature increased (right, 1780°C, 5 hours [no. 56022]). Photomicrographs by W. Wang; magnified 100×.

cient temperatures. Below 1550°C, the euhedral morphology generally remained unchanged (figure 9). Crystal faces and edges were clearly observable, and the only detectable variation occurred at the interface between the zircon inclusions and the host sapphire. At temperatures as low as 1400°C, portions of the interface between some zircons and the host sapphire became slightly turbid or frosted, though most of the body of the zircons remained clear and transparent. Some radiating fractures around inclusions also became frosted. Other zircon inclusions in the same sample, particularly smaller ones, showed virtually no visible changes. Heating at 1450°C and 1500°C did not intensify the degree of frosting of the inclusion boundaries, and many inclusions (close to two-thirds) remained as pristine as those in unheated sapphires.

When the temperature was increased to 1550°C, however, most of the zircon inclusions were noticeably affected, with the greater part of their surfaces frosted or turbid looking (figure 10, left). After heating at 1600°C, the zircon inclusions displayed even more distinct morphological variations (figure 10, center). While the overall outline remained fundamentally unchanged, the crystal faces and distinct interface with the host sapphire almost entirely disappeared. Most notably, the surfaces of nearly all the inclusions were strongly mottled and frosted. In only a few (~5%), did we observe isolated regions that were transparent and pristine-looking after heating at this temperature. When heated at 1680°C and above, the shapes of the inclusions became irregular, losing their euhedral outlines (figure 10, right). Development of melt aureoles, drip-like trails, and discoid fractures began at ~1730°C and intensified notably with increasing temperature up to the maximum of 1850°C (figures 11 and 12). These melt-filled fractures showed basically the same orientation within the sapphire host and were nearly parallel to each other. Dendritic quenched crystals of baddeleyite (see next two sections for phase identification) were rare (~5%) after heating at 1680°C but common (>50%) at 1730°C and above.

SEM-EDS Analysis. This is a powerful technique for detecting phase changes and their reaction products. Changes in some zircon inclusions occurred at temperatures as low as 1400°C. Subsolidus decomposition reactions (a chemical reaction in which one solid phase turns into two or more separate solid phases without any melting) dominated below 1550°C. At these temperatures, the reaction was usually limited to the outermost rims of the zircon inclusions and

Figure 12. At 1850°C, melt aureoles, drip-like trails, and discoid fractures were common. The variation in color in these inclusions is caused by the different colors of the host sapphires. Photomicrographs by W. Wang; magnified 100× (left [sample no. 56024]) and 55× (right [no. 56025]).

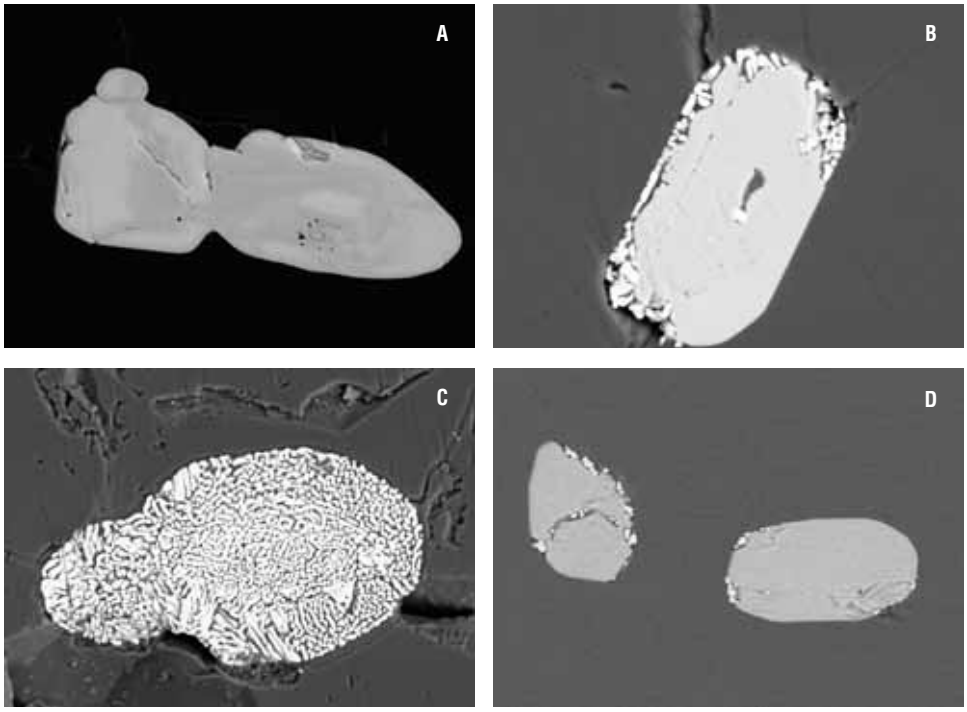

Figure 13. From 1400°C (A, B, C) to 1450°C (D), subsolidus decomposition reactions mainly occurred at the rims of some zircon inclusions, as seen in these backscattered electron images. The very bright areas are euhedral grains of baddeleyite (ZrO_2), which are surrounded by a dark, irregular SiO_2-rich phase containing up to 3 wt.% HfO_2. One zircon inclusion decomposed entirely (C). BSE image widths 180 μm (A); 80 μm (B); 160 μm (C); 140 μm (D).

involved the formation of two phases with extremely high contrast in the BSE images (figure 13). One inclusion showed no detectable reaction; in addition, it displayed clear growth zonation caused by variations of HfO_2 content in different regions (figure 13A). However, another inclusion in this sample was altered entirely, with no zircon surviving (figure 13C). Instead, very bright euhedral grains of baddeleyite (ZrO_2) were surrounded by a dark, irregular SiO_2-rich phase (refer to the Raman spectroscopy subsection below for phase identification and table 2 for chemical composition). The baddeleyite developed as small elongated euhedral crystals up to several micrometers in size. In contrast, the SiO_2-rich phase occurred as an interstitial material phase among baddeleyite crystals. The baddeleyite contained up to 3 wt.% HfO_2. Because of the very small grain sizes and strong overlap with surrounding minerals, we could not accurately determine the chemistry of the SiO_2-rich phase. Most of the interiors of individual zircon crystals remained unchanged. In general, the overall euhedral crystal outline of the inclusions was not disturbed. In a few cases, the reactions occurred internally but were limited in area.

The progression of these subsolidus decomposition reactions between 1400°C and 1550°C varied between samples and even between inclusions in the same sapphire. In sample nos. 75966 and 65458, which were heated to 1400°C and 1450°C, respectively, decomposition reactions were observed among a few isolated inclusions. Other zircons in the same sapphires showed no reaction at all (no. 75966), while one zircon inclusion in sample no. 75967 (heated to 1400°C) decomposed entirely (fig-

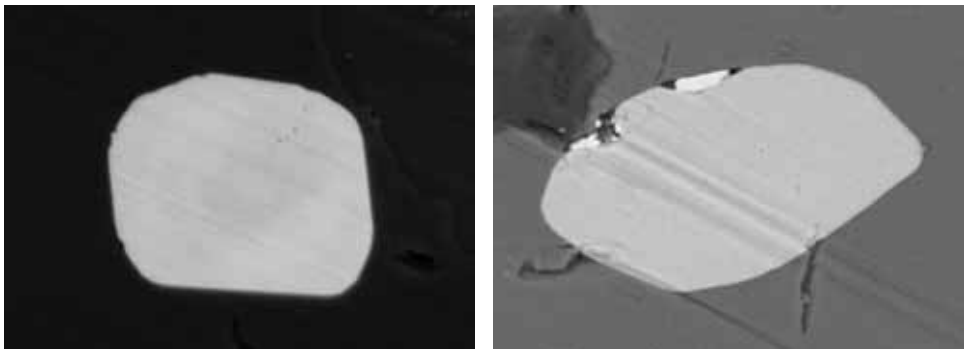

Figure 14. Some zircon inclusions heated to 1500–1550°C showed no observable changes (1500°C, left). Subsolidus reactions similar to those observed at 1400–1450°C (figure 13) were observed after heating at 1550°C (right). BSE image widths 20 μm.

Figure 15. When the zircon inclusions were heated to 1600°C, both subsolidus decomposition (left) and melting reactions (right) were observed. Heating for longer periods (25 hours, right) caused the formation of larger baddeleyite crystals, the brighter grains (compare to 5 hours, left). BSE image widths about 150 μm.

ure 13C). In contrast, none of the inclusions in sample nos. 65459 and 65461, which were heated to 1450°C and 1500°C, respectively, showed any observable changes (e.g., figure 14, left). A similar reaction to that occurring at 1400°C–1450°C was observed in one zircon inclusion after heating to 1550°C (no. 65463, figure 14, right).

After heating to 1600°C, both subsolidus decomposition and melting reactions were observed (figure 15). Sample no. 75968, which was heated for 25 hours, exhibited limited decomposition reactions along the rim of a zircon crystal, but the baddeleyite crystals that formed were larger (about 10 μm) than those seen after heating at lower temperatures and for shorter duration (2–3 μm; figure 15, left). Nevertheless, the euhedral morphology and outline of the original zircon were mostly preserved. Partial melting of a zircon inclusion occurred in sample no. 75969, which was also heated to 1600°C (figure 15, right). The melted inclusions consisted of baddeleyite crystals and Al_2O_3- and SiO_2-rich quenched melt. The original euhedral crystal outlines were indistinct.

Above 1680°C, partial melting occurred in nearly all the zircon inclusions (figure 16). In addition, the baddeleyite crystals within the Al_2O_3- and SiO_2-rich quenched glass matrix crystallized in a dendritic structure that was very different from the individual baddeleyite crystals that formed at lower temperatures. Reactions between the zircon inclusions and the host sapphire were intensified at temperatures at or above 1730°C, and the outlines of the original inclusions became difficult to discern (figure 17). Up to 5 wt.% HfO_2 was detected in baddeleyite in these melted inclusions. The melt (i.e., the quenched glass) was mainly composed of Al_2O_3 and SiO_2 with some ZrO_2 (up to 17 wt.%). The concentrations of Al_2O_3 and SiO_2 varied dramatically between different analysis locations. Average compositions of the melts are listed in table 2. Significant amounts of Na_2O, MgO, CaO, TiO_2, and/or K_2O were also detected in the melted portions of a few inclusions.

Infrared Absorption Spectroscopy. No absorption from either the zircon or the decomposition reaction products was detected by FTIR analysis after heating at any temperature. In addition, after heating in an oxidizing environment at high temperatures, most of the sapphire samples showed very little evidence of hydrogen. Of the 22 heated sapphires analyzed with FTIR, trace hydrogen was detected in only six. The intensity of the hydrogen absorption coefficient at 3309 cm^{-1} varied from 0 to 0.040 cm^{-1} (again, see figure 6). A very weak absorption at 3309 cm^{-1} was detected in sample no. 56017 after heating at 1600°C for 5 hours, but in a similar sample (no. 75968) heated at the same temperature for 25 hours, no hydrogen-related absorption was present. Notably, our heating experiments in oxidizing conditions did not result in the complete removal of structurally bonded hydrous components.

Raman Spectroscopy. In each of the heated samples, two to four inclusions were randomly selected for analysis. For sapphires heated at 1400°C and 1450°C,

Figure 16. When heated above 1680°C, nearly all the zircon inclusions showed some degree of melting, in addition to subsolidus reactions. In this inclusion, the quenched baddeleyite had a dendritic structure. BSE image width 85 μm.

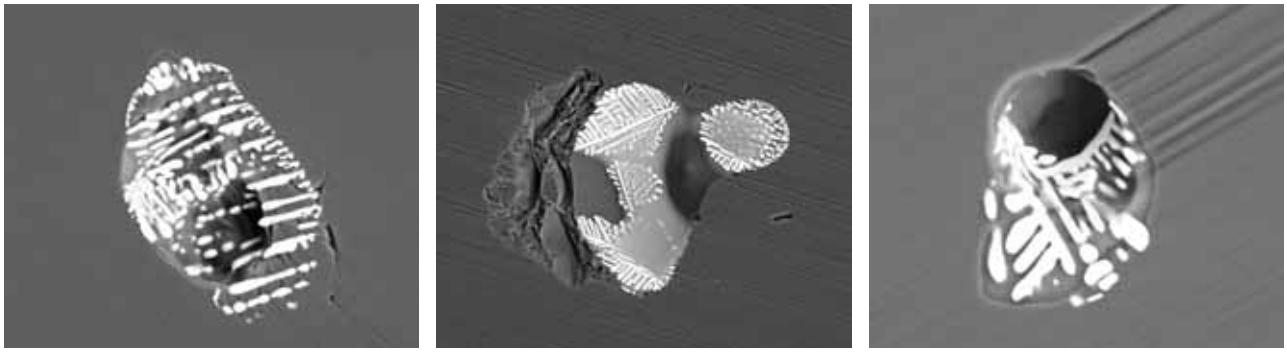

Figure 17. For temperatures at or above 1730°C, the outlines of the original zircon inclusions were diffused, and reactions between the inclusions and the host sapphire intensified (1730°C, left; 1780°C, center; 1850°C, right). Tiny dendritic-like quenched crystals of baddeleyite also formed, and the melt often penetrated into surrounding discoid fractures. BSE image widths 130 μm (left); 250 μm (center); 80 μm (right).

the inclusions displayed only the characteristic zircon Raman peaks, and no obvious differences from unheated zircon inclusions were observed. In samples heated to 1500°C and above, variations in Raman spectra were apparent. In the four inclusions analyzed in sample no. 65461 (1500°C for 5 hours), two inclusions showed at least seven additional emission peaks in the scattering region of 1300–1050 cm^{-1}, in addition to the dominant peaks from zircon when excited with a 514.5 nm laser (figure 18, top spectrum).

The characteristic zircon Raman peaks from most heated inclusions were shifted to higher wavenumbers (ν_3 = 1012–1021 cm^{-1}) compared to those observed for the natural free-standing single zircons, as was the case with the zircon inclusions in unheated sapphires. Raman peaks from zircon were the dominant features until melting occurred at ~1600°C. However, the FWHMs of the Raman peaks in the heated inclusions were significantly lower than those measured in the unheated zircon inclusions. For example, the average ν_3 FWHM for zircons that remained intact after heating was 8.7 cm^{-1} (1400°C), 8.5 cm^{-1} (1450°C), 8.4 cm^{-1} (1500°C), 7.9 cm^{-1} (1550°C), and 8.5 cm^{-1} (1600°C). In contrast, the average ν_3 FWHM for unheated zircon inclusions was 11.5 cm^{-1}.

The seven additional Raman peaks observed at 1500°C in sample no. 65461 were present in all inclusions heated at 1600°C and above. A secondary laser with 488 nm excitation confirmed that these peaks were due to luminescence and not the Raman effect.

The zircon-specific Raman peaks disappeared entirely from inclusions that were heated above 1680°C, and were replaced by several weak Raman peaks below 1050 cm^{-1} (figure 18, bottom spectrum). Of the more than 15 peaks that were recorded (not all of which are apparent in figure 18), several (645.5, 476.4, 396.5, and 336.4 cm^{-1}, and a characteristic doublet at 182.1 cm^{-1} and 194.4 cm^{-1}) were consistent with the Raman spectrum for baddeleyite (Stefanc et al., 1999; Fredericci and Morelli, 2000; McKeown et al., 2000), confirming its presence in the heated inclusions.

Figure 18. At least seven additional emission peaks in the 1300–1050 cm^{-1} scattering region due to luminescence were recorded for inclusions in a sample heated to 1500°C when 514.5 nm laser excitation was used (top). Most of these luminescence peaks were much stronger when the sample was heated at 1680°C or above. At wavenumbers less than 1020 cm^{-1}, there is a relatively weak spectrum for baddeleyite.

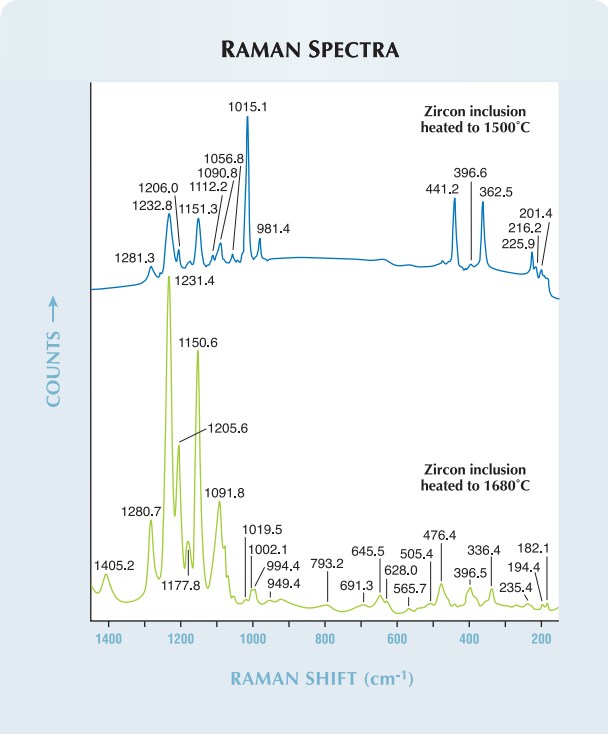

DISCUSSION

Raman Spectroscopy of Unheated Zircon Inclusions and Metamictization. Details of the Raman spectrum of zircon have been well known since the 1970s. The three main peaks at 1008, 974, and 439 cm^{-1} are related to internal SiO_4 vibration modes. It is generally agreed that the three other peaks at 225, 214, and 202 cm^{-1} are lattice vibrational modes involving interactions between SiO_4 tetrahedra and Zr atoms (Griffith, 1969; Syme et al., 1977).

As shown in figure 8, the Raman spectra from the zircon inclusions in unheated Madagascar sapphires were quite variable, particularly in the positions of the peaks. Shifting of peak ν_3 was as high as 13 cm^{-1}. The positions and relative intensities of Raman peaks are affected by many factors, including chemical composition, pressure, temperature, and crystallographic orientation. Analysis of the purple zircon crystal in multiple directions using 514.5 nm laser excitation demonstrated that relative peak intensity varied greatly with sample orientation. When the c-axis was parallel to the vibrational direction of the incident laser beam, the peaks ν_1 and ν_3 became very weak relative to other orientations, or they disappeared entirely. However, the peak *positions* showed virtually no change when the sample was in different orientations, as the largest shift was <0.5 cm^{-1}. These observations indicate that differences in crystal orientation most likely were not responsible for the shifting of Raman peaks observed in zircon inclusions from Madagascar sapphires.

We also considered whether these large peak shifts could be explained by HfO_2 substitution, since HfO_2 is a common minor oxide in zircon inclusions in Madagascar sapphires. In a careful study of Raman peak positions in synthetic end-member zircon ($ZrSiO_4$) and hafnon ($HfSiO_4$), Nicola and Rutt (1974) found that both had very similar Raman spectra, but the ν_3 peak position in hafnon was about 10 cm^{-1} higher than that of zircon, and the ν_1 and ν_2 peaks were also shifted to higher positions (9–10 cm^{-1}). In contrast, the 356 cm^{-1} peak in zircon ($ZrSiO_4$) occurred at 350 cm^{-1} in hafnon ($HfSiO_4$). Based on previous research (Hoskin et al., 1996), 3–5 wt.% HfO_2 in zircon is insufficient to cause the observed peak shift.

Thus, we do not believe that the large peak shifts that we observed (6–13 cm^{-1}; again, see figure 8) can be explained by either HfO_2 substitution or crystal orientation. Instead, the most likely scenario is that the zircon inclusions in Madagascar sapphires are confined under relatively high pressures. It has been well documented that Raman peaks for many minerals shift to higher wavenumbers with increasing pressure. The relationship between pressure and peak position is nearly linear, as observed from mineral inclusions in natural diamonds (see, e.g., Liu et al., 1990; Izraeli et al., 1999; Sobolev et al., 2000). When a zircon crystal is originally trapped within a newly formed sapphire at moderate temperatures (250°C–1400°C; G. Rossman, pers. comm., 2003), its volume is the same as the space it occupies in the host sapphire. However, the coefficient of thermal expansion of zircon ($3.2–5.4 \times 10^{-6}$/°C; Bayer, 1972) is lower than that of corundum (7.6×10^{-6}/°C; White and Roberta, 1983). Consequently, when the sapphire is brought to the earth's surface, where temperature and pressure are lower, differential expansion occurs between the inclusion and its host. The volume of the host sapphire and the original space the inclusion occupied decreases more than that of the zircon inclusion itself, placing the zircon under pressure and creating stress in the host sapphire surrounding the inclusion. Where the stress exceeds the tensile strength of sapphire, fractures develop (again, see figure 4). Similar features are common in natural diamonds with mineral inclusions. Knittle and Williams (1993) studied the Raman peak shifting of zircon under pressure at room temperature and found that the four major peaks (ν_1, ν_2, ν_3, 357 cm^{-1}) shifted positively and linearly. Based on their experimental results, the largest shift of the ν_3 peak in our data (13 cm^{-1}) corresponds to 27 kbar of pressure. Similar pressures were calculated from the shifting of other peaks.

Natural zircons also usually contain measurable amounts of radioactive trace elements. Radioactive decay of Th and U can damage zircon's crystal lattice, a process referred to as *metamictization*, which causes expansion of the zircon; this expansion can create internal stress (e.g., Guo et al., 1996; Hughes, 1997). Radiation damage also causes the Raman peaks of zircon to become less intense, broader, and to shift to lower wavenumber positions (Nasdala et al., 1995, 2003).

Raman peaks of pristine, unheated zircons in Madagascar sapphires were mostly strong and sharp, overlying a nearly flat background and shifted to higher wavenumbers (figures 7 and 8) than in free-standing and synthetic zircons. The observed shift to higher wavenumbers likely is a reconciliation of the compressive and tensile stresses caused by the competing mechanisms of thermal expansion and metamictiza-

tion. Even so, distinct radiation-related features were observed in these spectra. Crystalline zircon is a much better Raman scatterer than metamict zircon. As a result, the Raman spectra of metamict zircons are still dominated by peaks of crystalline zircon even with relatively high levels of radiation damage (Nasdala et al., 2003). Nasdala et al. (1995) found that the FWHM of the ν_3 peak was a very good indicator for metamictization in zircon. In a well-crystallized zircon, the ν_3 FWHM is less than 5 cm^{-1}. Partially metamict zircons commonly show FWHM values of more than 10 cm^{-1}, and highly metamict, X-ray amorphous samples have values ≥ 30 cm^{-1}.

The FWHM values of ν_3 from unheated zircon inclusions in this study were in the range 10.1–13.5 cm^{-1}, with an average of 11.5 cm^{-1}. These relatively high values strongly indicate that the zircon inclusions in the unheated samples were partially metamict. This conclusion is supported by the significant decrease of ν_3 FWHM after heating experiments. Average FWHM values for sapphires heated to 1400°C were 8.7 cm^{-1}, 8.5 cm^{-1} at 1450°C, 8.4 cm^{-1} at 1500°C, 7.9 cm^{-1} at 1550°C, and 8.5 cm^{-1} at 1600°C. We interpret this observed decrease to gradual recovery and repair of the radiation-damaged crystal structure through annealing at high temperatures.

All of these observations indicate that the zircon inclusions in the Madagascar sapphires were metamict to some extent. Radiation damage and differential thermal expansion during transport of the sapphires to the earth's surface most likely generated the radial cracks surrounding the zircons. However, differences in the radioactive trace-element composition of individual inclusions would result in varying degrees of metamictization. Thus, significant variations in internal stresses for different inclusions in the same sapphire would be anticipated. Indeed, large variations in ν_3 positions between sample nos. 75975 (ν_3 positions for three zircon inclusions = 1017.7, 1015.6, and 1008.1 cm^{-1}) and 76732 (ν_3 = 1015.1, 1014.8, and 1009.3 cm^{-1}) are probably the result of some combination of metamictization and differential thermal expansion.

Reactions of Zircon Inclusions at High Temperatures. Zircon inclusions experience a number of reactions and changes as they are exposed to increasing temperature (figure 19). Our microscopic observations, SEM-EDS chemical analyses, and Raman spectroscopy revealed that decomposition of zircon inclusions began at temperatures as low as 1400°C by the reaction: $ZrSiO_4$ (solid) → ZrO_2 (solid) + SiO_2 (solid). This subsolidus reaction involved no melting up to 1550°C. It is evident that the decomposition reaction was mostly limited to the rims of some zircon inclusions and did not occur for all of them. In rare cases, this reaction could occur throughout a whole inclusion, and no zircon survived in these inclusions. The reaction occurred exclusively in the zircon crystals, and the host sapphire was not involved. As a result, the overall morphology of the inclusions remained basically unchanged. However, the formation of tiny baddeleyite crystals and SiO_2-rich phases along the rims of some of the zircons significantly changed their reflective optical properties, giving the interfaces between the inclusions and host sapphire a frosty appearance (figures 9 and 10, left).

Both subsolidus and melting reactions were observed after heating at 1600°C. Decomposition reactions at this temperature (e.g., figure 15, left) were similar to those occurring at lower temperatures, except for the better crystallization of baddeleyite due to the higher temperature and longer periods of heating up to reach the target temperature. However, melting of zircon inclusions was observed in a few samples heated under these conditions (e.g., figure 15, right) following the reaction: $ZrSiO_4$ (solid) + Al_2O_3 (solid) → ZrO_2 (solid) + melt (liquid). Above 1680°C, all the zircon inclusions showed evidence of melting. High concentrations of Al_2O_3 in the melt (again, see table 2) provided ample evidence that the host sapphire was involved in the reaction at the highest temperatures. Melting of both the zircon inclusion and dissolution of the surrounding sapphire destroyed the original euhedral outline of these inclusions, producing irregular shapes. Widespread formation of tiny dendritic quenched crystals of baddeleyite caused the inclusion surfaces to appear severely mottled and frosted. Rapid volume expansion of the inclusions during melting generated high internal stresses, and caused the formation of discoid fractures in the surrounding sapphire. Zircon inclusions heated to these high temperatures may be identified by the presence of melt penetrating into the discoid fractures (again, see figures 11 and 12).

Through subsolidus and melting reactions due to heating at various temperatures, new phases are introduced into the original zircon-corundum system. Just as the IR absorption spectra of sapphires with zircon inclusions before heating experiments

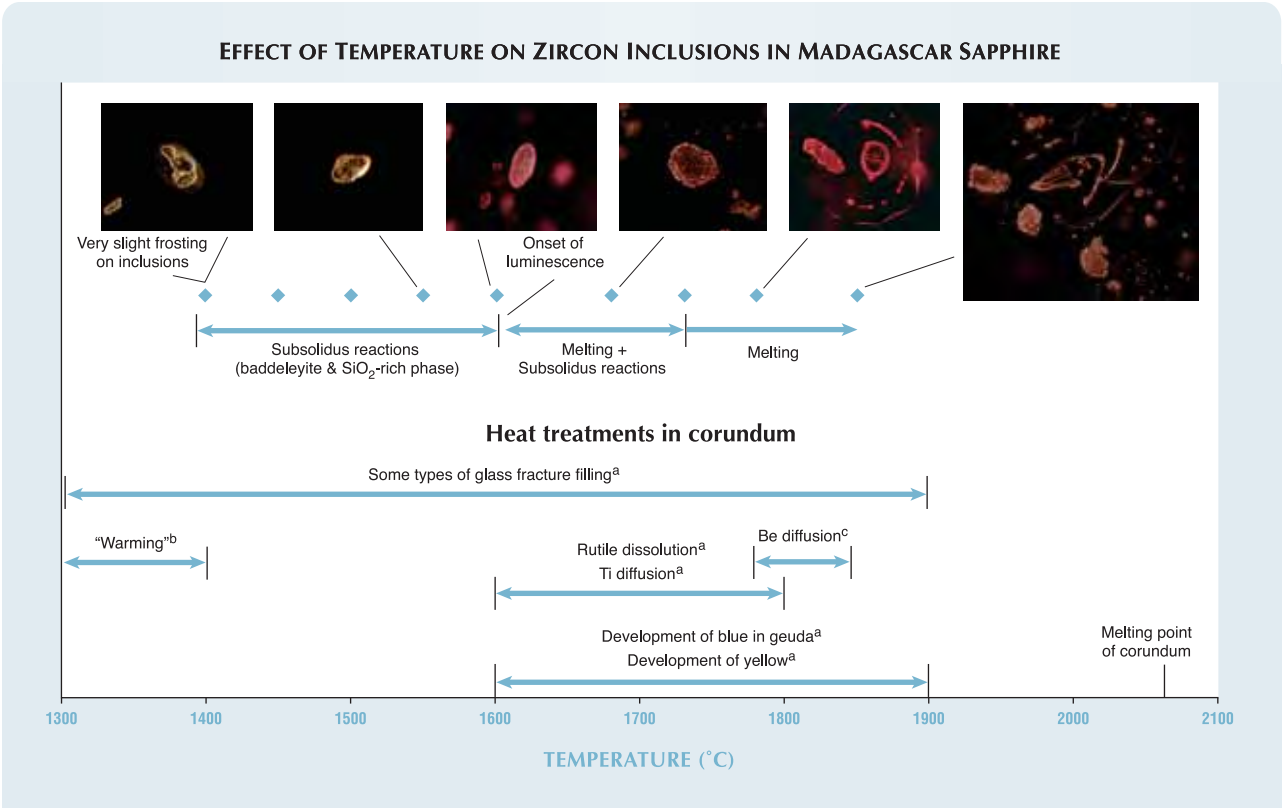

Figure 19. The morphology of zircon inclusions in the sapphires changed systematically as a function of heating temperature. Also shown are the general temperature ranges of common heat treatments. (References: [a]Hughes, 1997; [b]McClure et al., 2006; [c]Emmett et al., 2003.) Photomicrographs by W. Wang.

showed no zircon-related absorption, the IR absorption spectra of the heated samples did not show any features that could be attributed to reaction products. The main reason is that corundum has a strong absorption in the region below 1600 cm^{-1}, which masks any possible absorption in this region from reaction products. In addition, both the inclusions and the reaction products have a very limited volume compared to that of the host corundum, so the absorptions would be too weak to be detected even if they occurred above 1600 cm^{-1}. These observations indicate that IR absorption spectroscopy is not very sensitive in detecting the presence of minor amounts of zircon inclusions in corundum or its decomposition products after heating.

Lowered Melting Point of Zircon. Well-crystallized zircon is known to be stable up to 1690°C at ambient pressure (Nasdala et al., 2003). Above this temperature, it decomposes into the constituent oxides ZrO_2 and SiO_2. Zircon inclusions in sapphire form a simple $ZrSiO_4$–Al_2O_3 system, the lowest melting temperature of which should be 1700°C–1800°C (Budinikov and Litvakovskĭ, 1956). For the zircon inclusions in this study, both subsolidus and melting reactions started at much lower temperatures. The main possible causes for this discrepancy are radiation-related metamictization and the coexistence of other minerals mentioned below.

Internal structural damage from radiation could also affect the thermodynamic stability of zircon when heated. In an annealing study of radiation-damaged zircons (Zhang et al., 2000), it was found that heavily damaged samples tend to decompose into ZrO_2 and SiO_2 at high temperatures. In that study, tetragonal ZrO_2 was observed after annealing between 852°C and ~1327°C, while monoclinic ZrO_2 (baddeleyite) appeared above 1327°C. Such a decomposition temperature range is much lower than that for well-crystallized zircon. Zhang et al. (2000) also pointed out that ZrO_2 and SiO_2 from the decomposition could recrystallize to form new zircon around 1230°C.

All of these factors indicate that the final decomposition products of a zircon after heating would depend on the intensity of radiation damage, the annealing temperature, and the duration of heating.

This could explain the large variations in subsolidus decomposition for inclusions in individual sapphires, as well as the zircon decomposition observed at temperatures as low as 1400°C. There are two possible explanations for the pristine appearance of some zircon inclusions after the heating experiments: Either no decomposition occurred because they had experienced minimal radiation damage, or subsequent recrystallization occurred after decomposition. As seen in the Raman spectra, a few zircon inclusions showed the same peak positions as those of synthetic end-member zircon (figure 8), indicating that decomposition may not occur in all inclusions.

Although metamictization causes a dramatic decrease in the temperature at which subsolidus decomposition reactions begin, it is less likely to affect the melting temperature of this system. Melting of zircon inclusions in these Madagascar sapphires was first observed at 1600°C, more than 100°C lower than has been reported for a pure $ZrSiO_4$–Al_2O_3 system (Budinikov and Litvakovskĭ, 1956). Significant concentrations of MgO, CaO, K_2O, and TiO_2 were detected in the melted parts of a few inclusions (again, see table 2). Since all the samples were polished after heating to remove contamination, the most likely explanation is that these other minerals were originally present within or adjacent to the zircon inclusions. From the chemical composition of the melt, possible minerals include calcite, dolomite, magnesite, and/or feldspar.

Decomposition of zircon inclusions has also been reported in naturally heated corundum from Australian basalts (Guo et al., 1996). Similar to the studied sapphires, both partially reacted zircons and pristine inclusions were described in the same Australian corundum crystal. Guo et al. suggested that the presence of a SiO_2 phase with zircon inclusions would significantly decrease the melting point of the system. Unfortunately, extensive micro-Raman spectroscopic analysis of the unheated zircon inclusions failed to detect any signal from coexisting minerals. This is probably due to the sampling scale (μm) of Raman analysis and the uneven distribution of the coexisting minerals. In addition, small amounts of volatiles such as water and fluorine (undetectable with the spectroscopic and chemical techniques applied here), present as inclusions within or as a rim around the zircons, may also have a marked effect on decreasing the melting temperature of the $ZrSiO_4$–Al_2O_3 system.

Luminescence in the 542–552 nm Range. The presence of zircon decomposition reaction products was also detected through luminescence features in the 1300–1050 cm^{-1} (542–552 nm) range in the Raman spectra. Rankin and Edwards (2003) discovered at least seven emission peaks (514.5 nm laser excitation) in the 1300–1050 cm^{-1} region in zircon inclusions in extensively heated corundum crystals from Chimwadzulu Hill, Malawi. These peaks were thought to be due to luminescence from zircon decomposition reaction products, leading to speculation that they might be useful for correlation to high-temperature treatment of sapphire. Our study confirmed that these peaks were luminescent. In addition, we found that these peaks first appeared in two of the four analyzed zircon inclusions at 1500°C, and they were present in all of them after heating to >1600°C. The nature and source of the luminescence is unknown, but it is clearly not related to $ZrSiO_4$, because all of the zircon disappeared entirely after heating to >1680°C.

Applications for Gem Identification. Visual evidence of modification or destruction of solid inclusions in sapphire and ruby are powerful clues for determining if a stone has been heated. Experimental results from this study can be used to determine not only the possibility of heat treatment of sapphires with zircon inclusions, but also an estimate of the temperature applied (again, see figure 19). When some zircon inclusions (but not all) display limited frosted regions, well-preserved euhedral shapes, and only the characteristic zircon peaks in the Raman spectra, then the heating temperature is very likely ≤1450°C. With similar features seen under magnification but the occasional occurrence of luminescence peaks in the 542–552 nm region, the heating temperature might have reached 1500°C–1550°C. Heat treatment at ~1600°C might be identified by frosting of most of the zircon inclusion surfaces with the overall outline of the crystal remaining virtually unchanged; zircon features in the Raman spectra may or may not be detected when a stone has been treated at this temperature. If the zircon inclusions appear irregular and formless, but there is no evidence of melt-filled discoid fractures, the heating temperature was very likely around 1680°C. Treatment at this temperature also results in quenched dendritic crystals, a baddeleyite Raman spectrum, and strong luminescence in the 542–552 nm region. The presence of melt-filled

Figure 20. Many colors of Be-diffused sapphires (here, 0.5–2.0 ct) have been seen in the marketplace. The morphology of inclusions can supply useful information in determining if a sapphire should be tested further for the presence of Be. Photo by Elizabeth Schrader.

discoid fractures and halos with quenched dendritic crystals indicates that the heating temperature was >1730°C.

Any estimates of heating temperature must be based on careful observation of multiple zircon inclusions in a ruby or sapphire host. It is particularly important to examine multiple inclusions with samples that were possibly heated at <1550°C. Below this temperature, reactions involving zircon inclusions are very limited, and not all inclusions within a single stone will display the same features.

We feel this experiment could have particular application to the identification of Be diffusion in sapphires. Usually, trace-element chemical analysis (e.g., SIMS, LIBS, or LA-ICP-MS) is required to confirm if a stone is Be diffused. However, these instruments are expensive and not always available. Since treatment of Be diffusion in many cases requires a very high temperature (around 1800°C), the appearance of the zircon inclusions could be useful in estimating the heating temperature, assessing the need for trace-element analysis, and determining the color origin of sapphires and rubies.

CONCLUSIONS

Pristine zircon inclusions in Madagascar sapphires usually exhibit a euhedral crystal form and transparent interfaces with the host sapphire; occasionally, they have small sets of surrounding fractures. Most of the inclusions are under relatively high confining pressures due to differential thermal expansion and radiation damage related to their geologic history. Other minerals may coexist with zircon to form composite inclusions. The decomposition reaction and melting temperatures of these inclusions are apparently lower than they would be for a pure, well-crystallized $ZrSiO_4$–Al_2O_3 system. Microscopic and spectroscopic documentation of the systematic modification or destruction of zircon inclusions as a function of temperature provides a useful tool for determining whether a zircon-bearing ruby or sapphire has been heated, and for estimating the heating temperature.

Similar experimental studies are needed for other common mineral inclusions in ruby and sapphire to evaluate a wider range of heat-treatment conditions and to better constrain the temperature estimates. While these results may apply for the heat treatment of sapphires with zircon inclusions from localities other than Madagascar, a slight variation in the resulting modification or destruction of zircon inclusions is likely because metamictization significantly contributes to lowering the temperature of decomposition in these samples. Rubies and sapphires, including those from Madagascar, have historically been treated at a wide variety of temperatures: from very high, as with Be diffusion (figure 20), to lower temperatures than those examined in this study. To extend the possible usefulness of observed variations in zircon inclusions, similar heating experiments at 800°C–1400°C are ongoing.

ABOUT THE AUTHORS
Dr. Wang (wuyi.wang@gia.edu) is a research scientist at the GIA Laboratory, New York; Mr. Scarratt is director of Research at GIA Thailand, Bangkok; Dr. Emmett is a principal of Crystal Chemistry, Brush Prairie, Washington; Dr. Breeding is a research scientist at the GIA Laboratory, Carlsbad; Mr. Douthit is a principal of Crystal Chemistry, Los Altos, California.

ACKNOWLEDGMENTS
The authors are grateful to Matthew Hall, Shane McClure, Thomas Moses, Dr. Andy Hsi-Tien Shen, Dr. James Shigley, and Christopher Smith at the GIA Laboratory, and to Richard Hughes and John Koivula at the America Gem Trade Association Gemological Testing Center, for stimulating and helpful discussions. Dr. Chi Ma and Dr. George Rossman, of the California Institute of Technology, Pasadena, kindly provided assistance with the SEM-EDS analysis. Special thanks to Dr. George Rossman for the Raman spectrum of synthetic zircon.

REFERENCES

Bayer G. (1972) Thermal expansion of ABO_4 compounds with zircon and scheelite structures. *Journal of the Less-Common Metals*, Vol. 26, pp. 255–262.

Beesley C.R. (1982) The alchemy of blue sapphire. *Jewelers Circular Keystone*, Vol. 153, No. 8, pp. 102–103.

Budinikov P.P., Litvakovskĭ A.A. (1956) [title unknown]. *Doklady Akademia Nauk S.S.S.R.*, Vol. 106, p. 268.

Cozar J.S., de Vincente-Mingarro I. (1995) Alteración de las inclusiones de zircón, apatito y vidrio en el tratamiento térmico de rubíes y zafiros. *Boletín del Instituto Gemológico Español*. Vol. 36, pp. 47–54.

Crowningshield R. (1966) Developments and highlights at GIA's lab in New York: Unusual items encountered. *Gems & Gemology*, Vol. 12, No. 3, p. 73.

Emmett J.L., Douthit T.R. (1993) Heat treating the sapphires of Rock Creek, Montana. *Gems & Gemology*, Vol. 29, No. 4, pp. 250–272.

Emmett J.L., Scarratt K., McClure S.F., Moses T., Douthit T.R., Hughes R., Novak S., Shigley J.E., Wang W., Bordelon O., Kane R.E. (2003) Beryllium diffusion of ruby and sapphire. *Gems & Gemology*, Vol. 39, No. 2, pp. 84–135.

Fredericci C., Morelli M.R. (2000) Corrosion of AZS and AZ crucibles in contact with a blast-furnace slag-based glass. *Materials Research Bulletin*, Vol. 35, pp. 2503–2514.

Griffith W.P. (1969) Raman studies on rock-forming minerals. Part I: Orthosilicates and cyclosilicates. *Journal of Chemical Society (A)*, Vol. 1969, pp. 1372–1377.

Gübelin E.J. (1973) *Internal World of Gemstones*. ABC Verlag, Zurich.

Gübelin E.J., Koivula J.I. (1986) *Photoatlas of Inclusions in Gemstones*. ABC Edition, Zurich.

Guo J.F., O'Reilly S.Y., Griffin W.L. (1996) Zircon inclusions in corundum megacrysts: I. Trace element geochemistry and clues to the origin of corundum megacrysts in alkali basalts. *Geochimica et Cosmochimica Acta*, Vol. 60, No. 13, pp. 2347–2363.

Hoskin P.W.O., Rodgers K.A. (1996) Raman spectral shift in the isomorphous series $(Zr_{1-x}Hf_x)SiO_4$. *European Journal of Solid State Inorganic Chemistry*, Vol. 33, pp. 1111–1121.

Hughes R.W. (1997) *Ruby & Sapphire*. RWH Publishing, Boulder, Colorado.

Izraeli E.S., Harris J.W., Navon O. (1999) Raman barometry of diamond formation. *Earth and Planetary Science Letters*, Vol. 73, No. 3, pp. 351–360.

Knittle E., Williams Q. (1993) High-pressure Raman spectroscopy of $ZrSiO_4$: Observation of the zircon to scheelite transition at 300K. *American Mineralogist*, Vol. 78, No. 1, pp. 245–252.

Liu L.G., Mernagh T.P., Jaques A.L. (1990) A mineralogical Raman-spectroscopy study on eclogitic garnet inclusions in diamond from Argyle. *Contributions to Mineralogy and Petrology*, Vol. 105, No. 2, pp. 156–161.

McKeown D.A., Muller I.S., Buechele A.C., Pegg I.L., Kendziora C.A. (2000) Structural characterization of high-zirconia borosilicate glasses using Raman spectroscopy. *Journal of Non-Crystalline Solids*, Vol. 262, pp. 126–134.

McClure S.F., Smith C.P., Wang W., Hall M. (2006) Identification and durability of lead glass-filled rubies. *Gems & Gemology*, Vol. 42, No. 1, pp. 22–34.

Nasdala L., Wolf D., Irmer G. (1995) The degree of metamictization in zircon: A Raman spectroscopic study. *European Journal of Mineralogy*, Vol. 7, No. 3, pp. 471–478.

Nasdala L., Pidgeon R.T., Wolf D. (1996) Heterogeneous metamictization of zircon on a microscale. *Geochimica et Cosmochimica Acta*, Vol. 60, pp. 1091–1097.

Nasdala L., Zhang M., Kempe U., Panczer G., Gaft M., Andrut M., Plotze M. (2003) Spectroscopic methods applied to zircon. In J.M. Hanchar and P.W.O. Hoskin, Eds., *Reviews in Mineralogy and Geochemistry*, Vol. 53, Mineralogical Society of America, Washington DC, pp. 427–467.

Nicola J.H., Rutt H.N. (1974) A comparative study of zircon ($ZrSiO_4$) and hafnon ($HfSiO_4$) Raman spectra. *Journal of Physics C: Solid State Physics*, Vol. 7, pp. 1381–1386.

Rankin A.H. (2002) Natural and heat-treated corundum from Chimwadzulu Hill, Malawi: Genetic significance of zircon clusters and diaspore-bearing inclusions. *Journal of Gemmology*, Vol. 28, No. 2, pp. 65–75.

Rankin A.H., Edwards W. (2003) Some effects of extreme heat treatment on zircon inclusions in corundum. *Journal of Gemmology*, Vol. 28, No. 5, pp. 257–264.

Roberts R.B. (1975) Absolute dilatometry using a polarization interferometer. *Journal of Physics E*, Vol. 8, pp. 600–602.

Scarratt K. (1983) Heat treated sapphires. *Retail Jeweller*, Vol. 22, No. 543, pp. 16–17.

Schwieger R. (1990) Diagnostic features and heat treatment of Kashmir sapphires. *Gems & Gemology*, Vol. 26, No. 4, pp. 267–280.

Sobolev N.V., Fursenko B.A., Goryainov S.V., Shu J.F., Hemley R.J., Mao H.K., Boyd F.R. (2000) Fossilized high pressure from the earth's deep interior: The coesite-in-diamond barometer. *Proceedings of the National Academy of Sciences of the United States of America*, Vol. 97, No. 22, pp. 11875–11879.

Stefanc I.I., Music S., Stefanic G., Gajovic A. (1999) Thermal behavior of ZrO_2 precursors obtained by sol-gel processing. *Journal of Molecular Structure*, Vol. 480–481, pp. 621–625.

Syme R.W.G., Lockwood D.J., Kerr J. (1977) Raman spectrum of synthetic zircon ($ZrSiO_4$) and thorite ($ThSiO_4$). *Journal of Physics C: Solid State Physics*, Vol. 10, pp. 1335–1348.

White G.K., Roberts R.B. (1983) Thermal expansion of reference materials: Tungsten and α-Al_2O_3. *High Temperatures–High Pressures*, Vol. 15, pp. 321–328.

Zhang M., Salje E.K.H., Capitani G.C., Leroux H., Clark A.M., Schlüter J., Ewing R.C. (2000) Annealing of α-decay damage in zircon: A Raman spectroscopic study. *Journal of Physics: Condensed Matter*, Vol. 12, pp. 3131–3148.